Electronic band structure of magnesium and magnesium oxide: experiment and theory

1999 J. Phys.: Condens. Matter 11 7507

(http://iopscience.iop.org/0953-8984/11/39/308)

J. Phys.: Condens. Matter **11** (1999) 7507–7522. Printed in the UK PII: S0953-8984(99)04908-5

Electronic band structure of magnesium and magnesium oxide: experiment and theory

S A Canney†§, V A Sashin†, M J Ford† and A S Kheifets‡

† Physics Department, Flinders University of South Australia, GPO Box 2100, Adelaide, SA 5001, Australia

‡ Research School of Physical Sciences and Engineering, Institute of Advanced Studies, ANU, Canberra, ACT 0200, Australia

Received 2 June 1999

Abstract. Electron momentum spectroscopy (EMS) has been used to measure the valence band electronic structure of thin magnesium and magnesium oxide films. The band structures have also been calculated within the linear muffin-tin orbital (LMTO) approximation. The free-electron-like parabola characteristic of metallic solids was observed for magnesium with a bandwidth of approximately 6 eV, in agreement with previous measurements. The inclusion of energy broadening due to finite hole-lifetime effects and a Monte Carlo simulation of multiple scattering events gives good agreement between calculated and measured band structures. However, we measure a much higher intensity due to plasmon excitation compared with the simulated intensity. Upon oxidation the valence structure splits into two distinct, less dispersive bands typical of an ionic solid. Intensity due to plasmon excitation was almost completely absent in the experimental spectra for magnesium oxide. The LMTO calculation reproduces the overall structure and dispersion range of the oxide. The measured and calculated energy gap between upper and lower valence bands and their relative intensities do not agree quantitatively. This discrepancy may be due to a contribution of magnesium s states to the predominantly oxygen p states in the upper band.

1. Introduction

Magnesium lies very close to being a free-electron-like metallic solid with only a very weak bulk crystal potential. The valence band electronic structure is expected to closely resemble a free-electron-like parabola. In contrast, magnesium oxide is close to an ideal insulating ionic solid with a valence band structure dominated by the strong potential of the ionic cores. The different chemical bonding and electronic structure exhibited by these two systems provides an opportunity to test the applicability of theoretical models to two extreme examples of the solid state.

Measurements of the electronic properties of these materials, particularly MgO, are also motivated by their technological applications, for example in catalysis, microelectronics and electrochemistry. MgO has been more widely studied both experimentally [1–3] and theoretically [4–6] compared to metallic magnesium. There is, however, a lack of experimental measurements of the band structures of either Mg or MgO reported in the literature, presumably due to the experimental difficulties in applying techniques such as photoemission to these systems. Mg, with a valence band structure derived mainly from 3s states, has a small photoemission cross-section and oxidizes rapidly even under ultra-high vacuum (UHV)

§ Present address: Defence Science and Technology Organization, PO Box 1500, Salisbury, SA 5108, Australia.

0953-8984/99/397507+16$30.00

conditions [7]. The oxide, being an insulator, poses problems from the point of view of sample charging during photoemission measurements. Discrepancies still exist between various measurement techniques and theoretical calculations regarding the exact details of the electronic structures of these two systems.

The full energy–momentum resolved band structure is a fundamental quantity that has direct bearing upon the physical, chemical and electronic properties of a material. There is good cause for determining band structures experimentally in order to test reliability of our theoretical descriptions and predictions of solid-state properties. The use of photo-electron techniques such as angle resolved photoemission spectroscopy (ARPES) requires certain assumptions to be made about the state of the outgoing photo-ionized electron [8] in order for the band structure to be extracted from the measured energy profiles. This poses no great problem for solid targets that can be prepared with a well defined crystal structure [9]; however its application to amorphous or polycrystalline samples is limited. To the authors' knowledge there are no reported measurements of the full band structure of MgO.

Electron momentum spectroscopy (EMS) has been used with great success to map the electron momentum-space wavefunction in atomic and molecular targets [10]. The technique is equally applicable to the solid state where it measures directly the energy–momentum density [11], in other words the probability of finding an electron with a particular binding energy and momentum. EMS is complementary to photoemission techniques and, although it cannot yet achieve the energy resolution or short data collection times of ARPES, its ability to measure band structures of amorphous and polycrystalline, as well as crystalline, solids has clearly been demonstrated [12–15].

In this paper we report our EMS measurements of the valence band structures of polycrystalline thin films of Mg and MgO, together with calculated band structures within the linear muffin-tin orbital approximation. These two samples represent simple and almost ideal examples of metallic and ionic solids respectively and provide stringent tests of theory at the two extremes of chemical bonding. A comparison between the EMS results of magnesium oxide with theoretical calculations will also hopefully provide further information about discrepancies that arose in previous EMS measurements of aluminium oxide [15] and silicon dioxide [13]. Details of our electron momentum spectrometer and sample preparation techniques are described in the next section, section 2, followed by a description of the LMTO calculation in section 3. Experimental and calculated band structures are presented and discussed in section 4, followed by concluding remarks in section 5.

2. Experimental details

2.1. Electron momentum spectrometer

Electron momentum spectroscopy uses electron-impact ionization to map the electronic structure of an atomic, molecular or solid target. The underlying principle is essentially the same in all three cases. A high-energy incident electron of well defined energy E_0 and momentum $\boldsymbol{p}_0$ ionizes the target producing scattered incident and ejected target electrons. The momenta and energies of the two outgoing electrons are measured and the kinematics of the collision are then completely specified. In our experimental set-up we denote the energy and momentum of the fast scattered electron by E_f and $\boldsymbol{p}_f$ and those of the slow ejected electron by E_s and $\boldsymbol{p}_s$. If the momentum transferred from the incident electron to the target, $\boldsymbol{K} = \boldsymbol{p}_0 - \boldsymbol{p}_f$, is large, the ionization event can be described as a direct knock-out of the target electron—the so-called (e,2e) event [11]. Conservation of energy and momentum then allows us to determine

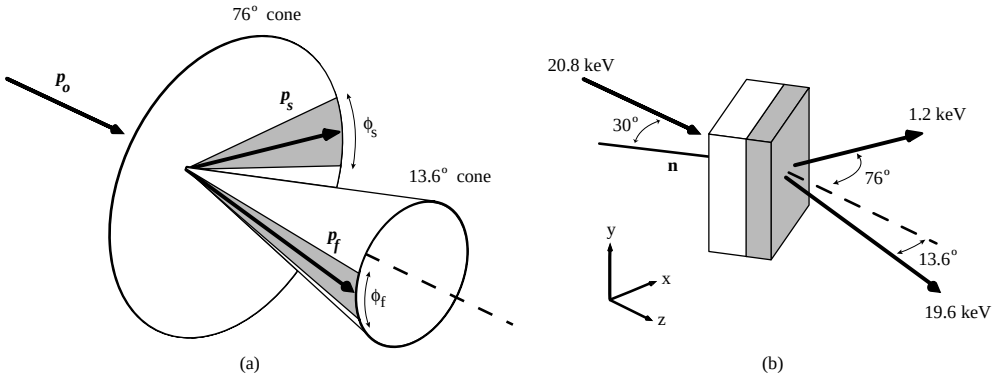

Figure 1. Schematic diagram of the experimental geometry. In (a) the range of detected electron angles is shown and in (b) sample orientation with respect to the incident and outgoing electrons is shown. The shaded area in (b) indicates the region of the sample that contributes most to the measured energy–momentum density.

the binding energy ε and momentum $\boldsymbol{q}$ of the target electron immediately *before* the collision:

$$\varepsilon = E_0 - E_s - E_f \qquad \boldsymbol{q} = \boldsymbol{p}_s - \boldsymbol{K}.$$

A coincidence detection method is used where the time correlation between the outgoing electrons is measured. Electrons originating from the same (e,2e) event will essentially arrive at the detectors at the same time. This allows us to extract the small signal from single-ionization events from a large background of other scattering processes and to discriminate pairs of electrons originating from the same ionization event from random pairs. By measuring the joint distribution of the outgoing electrons as a function of their energies and scattering/ejection angles we can map directly the probability density of the target electrons (the square of the electronic wavefunction) in energy–momentum space. This not only gives us the band structure of a solid target but also the ground state occupation of the bands.

The (e,2e) spectrometer used for our measurements has been described in detail elsewhere [16]. An asymmetric geometry is used with typically an incident energy of 20.8 keV, a fast scattered energy of 19.6 keV and a slow ejected energy of 1.2 keV. A schematic representation of the geometry is shown in figure 1(a). The polar angles of the outgoing scattered and ejected electrons are fixed by detecting them on the surface of 13.6 and 76° cones respectively. By varying the azimuthal angles ϕ_s and ϕ_f and energies at which the outgoing electrons are detected, the target-electron's binding energy ε and momentum distribution $\boldsymbol{q}$ are mapped. Each electron analyser is equipped with a two-dimensional position sensitive detector mounted at the exit aperture enabling a range of azimuthal angles and energies to be measured in a single experiment. The range of angles and energies detected is such that the energy–momentum density is measured along the y-axis indicated in figure 1. Hence, our apparatus has the capability of measuring band structures along definite crystal directions.

The relatively small escape depth of the slow ejected electron means that the measured (e,2e) signal comes from the outermost 2 nm of the target facing away from the incident beam, figure 1(b). This is a particularly useful feature as it allows us to prepare samples by evaporation onto a thin graphite substrate without the substrate contributing to the measured band structure. Scattering events that occur deeper within the target contribute to a background in the measurement. The background arises due to the incoming or outgoing electrons undergoing additional small-angle elastic or inelastic collisions within the target. Multiple scattering events produce a random component where essentially all energy–momentum information of

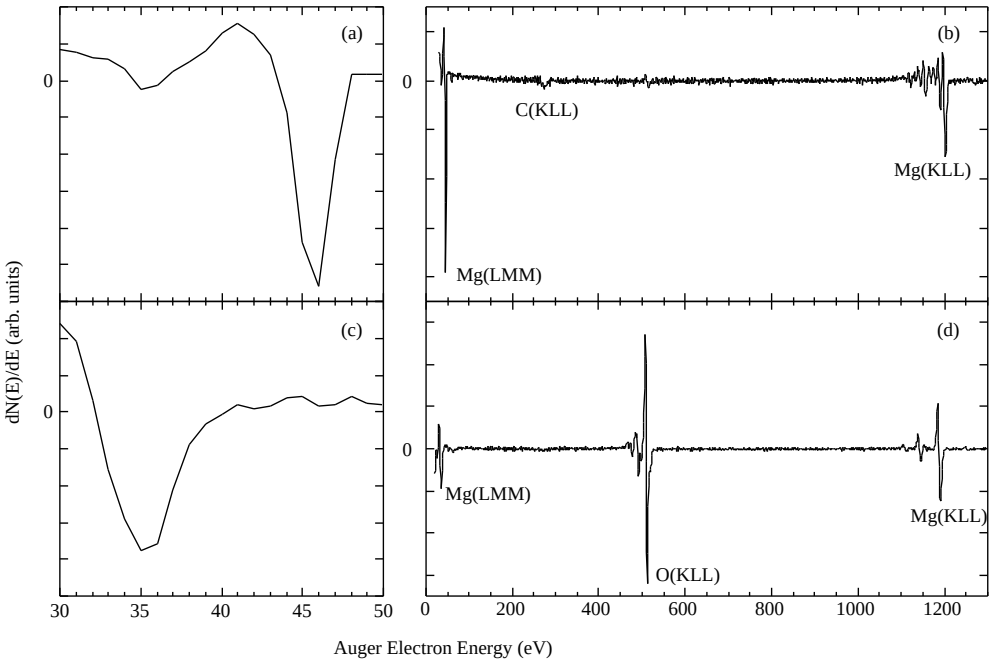

Figure 2. Differential Auger electron spectra for (a), (b) the Mg sample, and (c), (d) the oxidized Mg sample.

the target electron is lost and a structure that arises from excitation of plasmons by the incoming or outgoing electrons. Since plasmon excitation represents an additional energy-loss process it produces 'ghost' images of the band structure shifted by multiples of the plasmon energy. Performing the measurements in transmission means that the overall target thickness must be very small otherwise the (e,2e) signal is dominated by the multiple scattering background. In practice we find that the maximum acceptable sample thickness is of the order of 10 nm.

2.2. Sample preparation

Magnesium samples were prepared by evaporating a 7 nm layer of Mg onto a thin amorphous carbon substrate (3 nm) under ultra-high vacuum (UHV) conditions. Immediately after evaporation *in situ* Auger electron spectroscopy was performed on the sample to check the surface composition of the evaporated Mg layer. The resultant Auger spectra in figures 2(a) and (b) show a dominant contribution from the Mg layer. A small carbon peak was detected but more importantly there was no sign of surface oxidation. The presence of carbon could be due to either the underlying substrate or contamination during the evaporation process. It is important to note that because EMS measures the average band structure over the outermost 2 nm of the sample it is not very sensitive to carbon contamination on the surface. It is expected that Mg films produced with the above method are polycrystalline and that the Mg will possibly form islands on the carbon substrate [1]. Our (e,2e) results indicate that Mg covers the majority of the carbon surface since we see no evidence of carbon in our measured band structure. Even under UHV conditions the Mg layer oxidizes considerably over the three day period required to produce sufficient statistics in our (e,2e) measurement. In order to eliminate this problem, data were taken for three independent magnesium samples (with each sample run for 24 hours)

and the three sets of data were added together. Even though there is still some oxidation of the Mg surface after only one day it is not sufficient to be detected in the (e,2e) measurement.

Stoichiometric MgO films were prepared by Corneille *et al* [17] by evaporating metallic magnesium in the presence of oxygen onto an Mo(100) surface. We have followed a similar technique to produce our magnesium oxide samples. Samples were prepared by evaporating 5 nm of metallic magnesium onto a thin amorphous-carbon substrate, in an oxygen background of 1.0×10^{-6} Torr. It is claimed that samples produced in this manner appear to be much more homogeneous than an evaporated Mg layer that is later exposed to an oxygen environment (post-oxidation). We performed EMS measurements on samples prepared by both techniques to confirm this claim. The post-oxidation samples still show some metallic character in the band structure, whereas none is observed in the samples prepared by evaporation in an oxygen atmosphere. The Auger spectrum from a magnesium oxide sample is shown in figure 2(c) and (d). The dominant oxygen peak, together with the two magnesium peaks, clearly indicates that the sample has been oxidized. The metallic magnesium peak has also shifted from 46 eV (figure 2(a)) down to 35 eV (figure 2(c)) indicating the presence of Mg in an oxide environment [18].

3. Calculation

3.1. Magnesium

In our band structure and electron momentum density (EMD) calculations we used the LMTO method in the atomic sphere approximation (ASA) as described by Skriver [19]. The radii, R, of the two muffin-tin spheres representing two non-equivalent atomic positions of the hexagonal close-packed (HCP) structure can be estimated by equating the volume of the spheres to that of the unit cell:

$$R = \frac{\sqrt{3}}{2}\left(\frac{c}{a}\frac{1}{2\pi}\right)^{1/3}$$

where, according to Wyckoff [20], the lattice constants are $a = 3.21$ Å and $c = 5.21$ Å. The technique for deriving the energy–momentum density from the LMTO method is analogous to that reported for aluminium [14].

Results of the band structure and EMD calculations for Mg are presented in figure 3. Here we show our calculations in three major high symmetry directions of the HCP structure: Γ–K, Γ–M, Γ–A. As the experiment is performed on a polycrystalline sample a rigorous spherical averaging technique is implemented in our computation scheme. However, for a qualitative analysis, we expect the spherical average to be close to an arithmetic average of the three major high symmetry directions.

The band structure of Mg is different in all three directions but only one band contributes to the EMD at a given momentum. The sequence of contributing bands forms a continuous nearly free-electron parabola that is interrupted at the Brillouin zone boundary. The total momentum density is rather flat as one would expect for a nearly free-electron solid. These features are quite isotropic and would survive the spherical averaging, they should therefore be observable in the experiment. After being terminated at the Brillouin zone boundary, the EMD in the Γ–M direction reappears at a higher momentum. This feature does not exist in other directions and we do not expect it to be observed in our experiment performed on a polycrystalline sample.

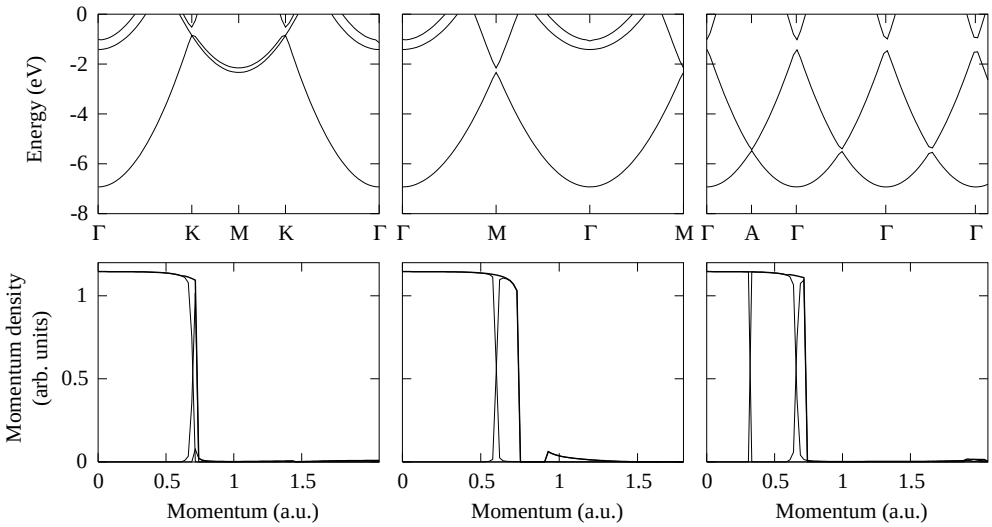

Figure 3. Band structures (top row) and electron momentum densities (bottom row) for Mg calculated within the LMTO approximation along several high symmetry directions. The thick solid line indicates electron momentum densities summed over all bands.

3.2. Magnesium oxide

Magnesium oxide has a face-centred cubic (FCC) unit cell with two non-equivalent atomic positions. The muffin-tin radius, R, is evaluated as

$$R = \frac{a}{3}\left(\frac{3}{\pi}\right)^{1/3} a$$

where, according to Wyckoff [20], the lattice constant is $a = 4.211$ Å.

The band structure and EMD for MgO are presented in figure 4 along the three major high symmetry directions Γ–X, Γ–K, and Γ–L. These are fairly representative for the FCC structure and the rigorous spherical average should be not be too different from the arithmetic average of the three directions.

The electronic structure of the valence band of magnesium oxide can be described by considering a simple ionic picture of the molecular unit MgO. In a purely ionic picture MgO is formed when charge is transferred between magnesium and oxygen atoms resulting in an Mg^{2+} cation and O^{2-} anion. Both Mg^{2+} and O^{2-} then have identical closed shell configurations, $1s^2 2s^2 2p^6$. The 2p and 2s electrons are more strongly bound to the nucleus in magnesium and hence the binding energies of the 2s and 2p electrons in Mg^{2+} are greater than in O^{2-}. The outermost orbitals of MgO are essentially comprised of the 2s and 2p orbitals associated with the oxygen atoms. The upper valence band of magnesium oxide is dominated by the oxygen ion 2p orbitals, whilst the lower valence band is dominated by the oxygen ion 2s orbitals.

The EMD of the lower valence band closely resembles that of the atomic 2s orbital and has maximum intensity at zero momentum. In contrast, the upper band near zero momentum has predominantly p character and therefore the EMD is vanishing. It picks up intensity away from the Γ point. The upper valence band comprises three individual bands that collapse to two bands in Γ–X and Γ–L directions. Of these two bands only one contributes to the EMD in these directions, whereas the contribution switches from one band to another in the Γ–K direction. Despite a visible difference in structure of the upper valence band, those bands

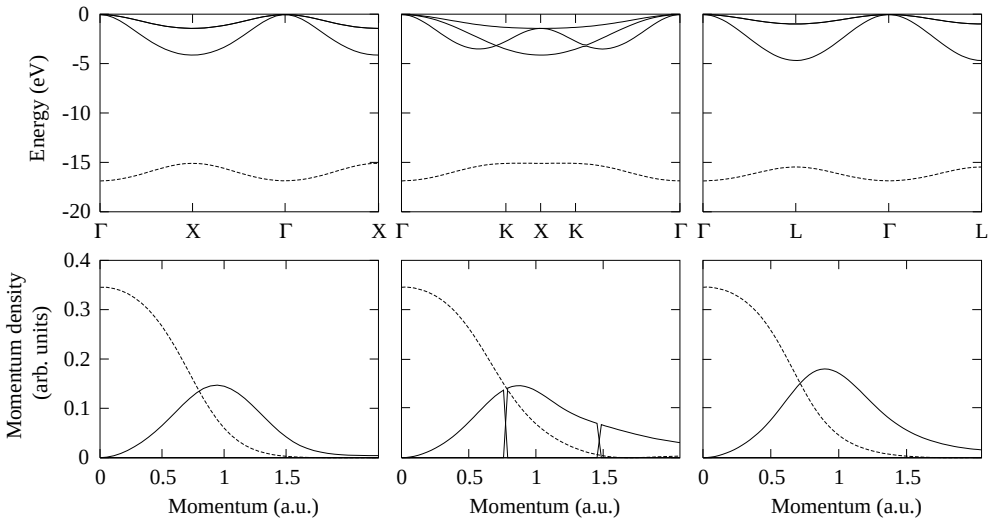

Figure 4. Band structures (top row) and electron momentum densities (bottom row) for MgO calculated within the LMTO approximation along several high symmetry directions. The dashed line indicates the low predominantly oxygen 2s band. The solid lines show the upper band.

contributing to the EMD form a fairly isotropic downward dispersing structure that should withstand spherical averaging and be prominent in our experimental results.

4. Results and discussion

4.1. Magnesium

The measured energy–momentum density for magnesium is shown in figure 5(a). This plot is the result of summing together three separate samples each measured for a period of one day. The band structure is plotted in terms of electron momentum rather than wavenumber because the EMS experiment measures the real momentum of the target electron rather than its crystal momentum. The expected free-electron parabolic dispersion curve can clearly be seen above the background, indicating that metallic magnesium had resulted from our measurement procedure. The magnesium sample is polycrystalline and as a result we measure a spherical average of the band structure over all crystal directions. It should be noted that the binding energy in this plot is referenced to the vacuum level, not the Fermi level as is the case in other experimental techniques.

For comparison, the result of the LMTO calculation that has been spherically averaged is also shown in figure 5(b). The theoretical result has been shifted by 5 eV to align the Fermi level (reference point for the calculation) with the vacuum level and has been convoluted with gaussians of 1.0 eV (FWHM) and 0.1 au (FWHM) to match the experimental resolutions. Bartynski *et al* [21] have reported an angle resolved photoemission study of the electronic structure of Mg(0001). In this measurement the width of the bulk binding energy peak as a function of reduced momentum was about 2.3 eV and remained fairly constant along the band. This width results from contributions of the electron and hole lifetimes. To account for lifetime broadening we have also convoluted the LMTO result with a Lorentzian. A Lorentzian of 1.8 eV (FWHM) gives good agreement between the measured and calculated bandwidths and intensities. Lifetime effects were also found to be important in the EMS measurements of aluminium [14].

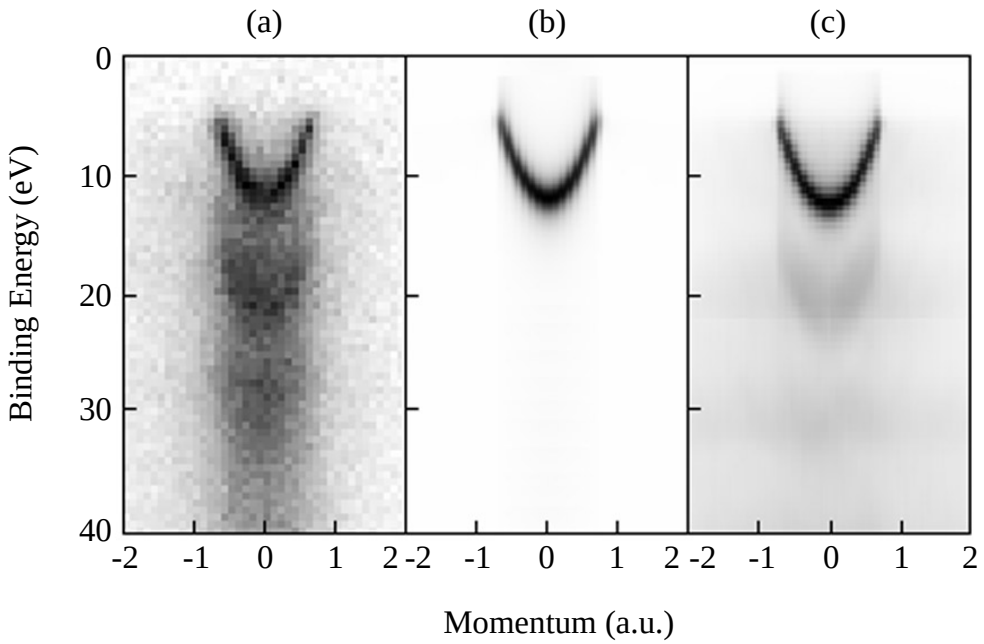

Figure 5. Energy resolved momentum densities for Mg, (a) measured by EMS, (b) calculated within the LMTO approximation and convoluted with the experimental resolutions and energy broadening due to lifetime effects and (c) simulated using a Monte Carlo procedure taking the LMTO calculation as input. Intensity is on a linear grey scale with darker colour representing higher intensity.

Intensity is also measured inside the free-electron parabola and at higher binding energies that is not predicted by the LMTO calculation. This intensity arises from multiple scattering events that are not taken account of in the calculation. We have employed a Monte Carlo simulation to add these effects into the LMTO calculation [22]; the results are also shown in figure 5(c). The simulation qualitatively reproduces multiple scattering features present in the measurement, i.e. a second parabola shifted by 10 eV and intensity inside the free-electron parabola at low momenta. The former arises from plasmon excitation, and the latter from small angle elastic scattering.

For a quantitative analysis the energy–momentum densities from the measurement, LMTO calculation and Monte Carlo simulation have been integrated over 0.1 au momentum intervals. The resultant binding energy profiles are shown in figure 6. Positive and negative momentum components have been added in this figure since the energy–momentum density should be symmetric about zero momentum. Intensities of the measured and calculated valence-band binding-energy peaks have been normalized for the momentum range $0.2 < q < 0.3$ au. The measurement shows a peak for the valence band of magnesium at 11.5 eV (for zero momentum) which disperses towards lower binding energies as the momentum increases. The total dispersion range (bandwidth) measured is approximately 6 eV. The LMTO calculation follows this dispersion very closely and gives a bandwidth of approximately 6.6 eV. Our measured bandwidth compares very well to the value of 6.15 eV measured by Bartynski *et al* [21] for single-crystal magnesium. Early band structure calculations revealed a width of 7 eV [23]. More recent calculations that utilized self-consistency predict a bandwidth of 6.9 eV [24, 25] whilst our LMTO calculation gives a somewhat smaller value. The observed width of

the valence-band peak and that predicted by the LMTO calculation after convoluting for finite experimental resolutions and lifetime effects are in good agreement.

The intensities of the valence band peak also agree very well, except around zero momentum where the LMTO calculation and Monte Carlo simulation show additional intensity. The measurement shows two additional peaks that follow the dispersion of the valence band shifted by about 10 and 20 eV. They are the result of electrons involved in an (e,2e) event exciting one or two plasmons respectively. The Monte Carlo procedure reproduces the plasmon features; however the simulated intensity is about 2 to 2.5 times lower than that measured. This discrepancy in the background at higher binding energies is identical to that seen for aluminium [14]. In this case, better agreement was obtained by including correlation effects in the calculation using cumulant expansion techniques [26]. Correlation effects are also expected to be important in magnesium.

4.2. Magnesium oxide

The measured energy–momentum density for magnesium oxide is shown in figure 7(a). Since the oxide is an ionic crystal a free-electron description of the band structure is no longer expected to be valid. This is immediately evident in the figure where the electronic structure has changed completely compared with the results in the previous section. Contributions from metallic magnesium are indeed no longer visible; neither are any contributions from the underlying amorphous carbon substrate. This provides further evidence that the sample preparation produces homogeneous oxide films, at least to the thickness of the sampling depth of our spectrometer ($\approx$2 nm). It is well recognized that when going from metallic magnesium to magnesium oxide the valence band splits into an upper and lower band separated by an inter-band gap. These features can clearly be seen in figure 7(a). There is a further noticeable difference between the metallic and oxide band structures: the latter shows a much smaller background due to inelastic scattering compared with the metallic case.

The calculated energy–momentum density of MgO is presented in figure 7(b) convoluted for the experimental energy and momentum resolution and shifted by approximately 8 eV to account for the measured energies being relative to the vacuum level. Once again the spherical average has been plotted to account for the polycrystalline nature of our sample. Qualitative agreement is seen between experiment and calculation for the dispersion of both valence bands. For a more detailed comparison binding energy profiles integrated over 0.2 au momentum intervals are plotted in figure 8. The positive and negative momentum components have been combined to improve the statistics. The calculated and measured intensities of the lower valence band peak have been normalized in the momentum range $0 < q < 0.2$ au. We have not attempted to include the effects of lifetime broadening or multiple scattering in the calculation. Lifetime effects were calculated for Mg using a free-electron gas theory which is not applicable to MgO. We are currently developing our Monte Carlo program to deal with films containing more than one atomic species.

The observed lower-valence bandwidth of approximately 1.5 eV compares well with the calculated dispersion range which is about 2 eV. In addition the intensity of this band is in good agreement up to a momentum of about 0.8 au. Both the measurement and calculation produce maximum intensity at zero momentum, with the intensity decreasing as the momentum increases. However, the observed lower band extends out to larger momentum values compared with the calculation. For the upper valence band, the measurement shows a broad peak at approximately 10 eV binding energy (in the momentum range $0 < q < 0.2$ au). This peak increases in intensity as the momentum increases reaching a maximum at about 0.8 au. The LMTO calculation displays a similar overall behaviour.

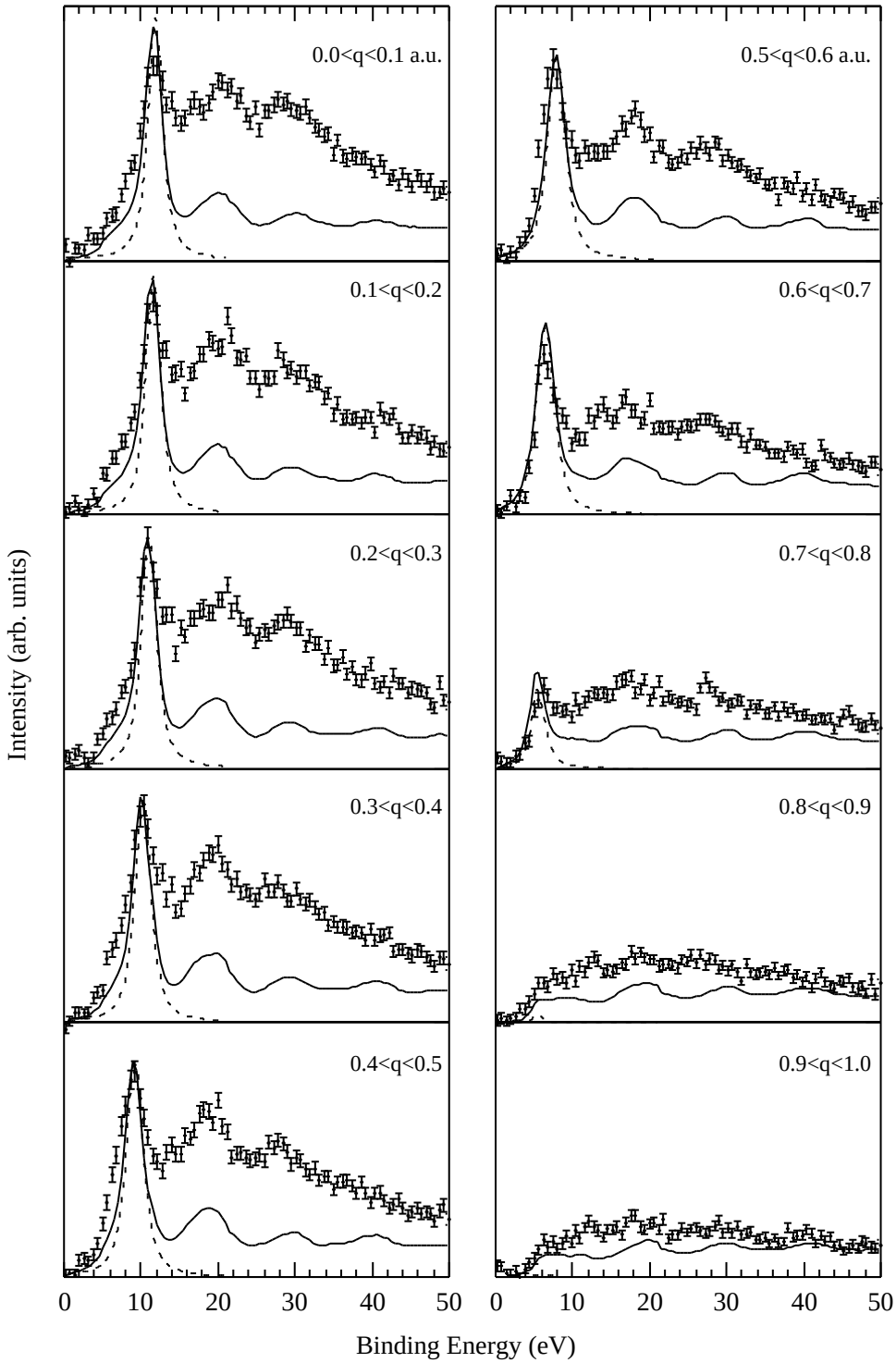

Figure 6. Binding energy profiles for Mg averaged over 0.1 au momentum intervals for the EMS measurement (points with error bars), the LMTO calculation (dashed line) and Monte Carlo simulation (solid lines).

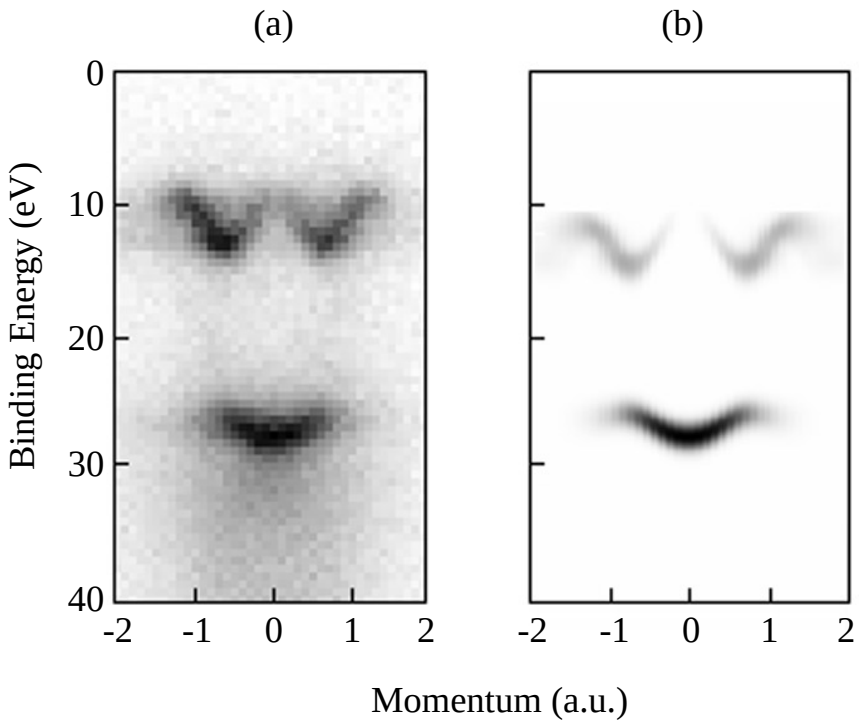

Figure 7. Energy resolved momentum densities for MgO, (a) measured by EMS and (b) calculated within the LMTO approximation and convoluted with the experimental resolutions. Intensity is on a linear grey scale with darker colour representing higher intensity.

There are a number of striking differences between observed and calculated band structures which deserve further attention: firstly, the relative intensities of the upper and lower bands, particularly at small momentum values; the calculation predicts virtually no intensity in the upper band compared with the observed intensity which is almost half that of the lower band; secondly, the relative positions of the two bands, or inter-band gap which is consistently 3 eV less in the calculation than the observed value; and finally the much larger width of the observed binding-energy peaks compared with calculation even after convoluting with the experimental resolution. This last point would indicate that lifetime effects are also important in MgO.

In a very simplistic ionic picture of MgO the band structure should exhibit energy levels associated with the 2s and 2p orbitals of oxygen that are non-dispersing. It is clear from figure 7 that in both the experiment and calculation the upper and lower valence bands do indeed disperse in energy as the momentum changes. This is because the orbitals are not localized and there is considerable overlap between neighbouring ions. Despite this fact, we might still expect the lower valence band to be dominated by 2s orbitals on the oxygen anion and the upper band by oxygen 2p orbitals. The calculated band structure supports this simple picture. The lower band shows maximum intensity at zero momentum monotonically decreasing with increasing momentum—characteristic of an s orbital. While the upper band is characteristic of a p orbital, i.e. maximum intensity at non-zero momentum with almost no intensity at zero momentum. It is generally assumed that the upper valence band is derived predominantly from O 2p with some bonding from Mg, see for example Henrich and Cox [27]. The relatively large intensity measured in the upper band at small momentum may originate from the contribution of s orbitals on the Mg cation which are not adequately described by

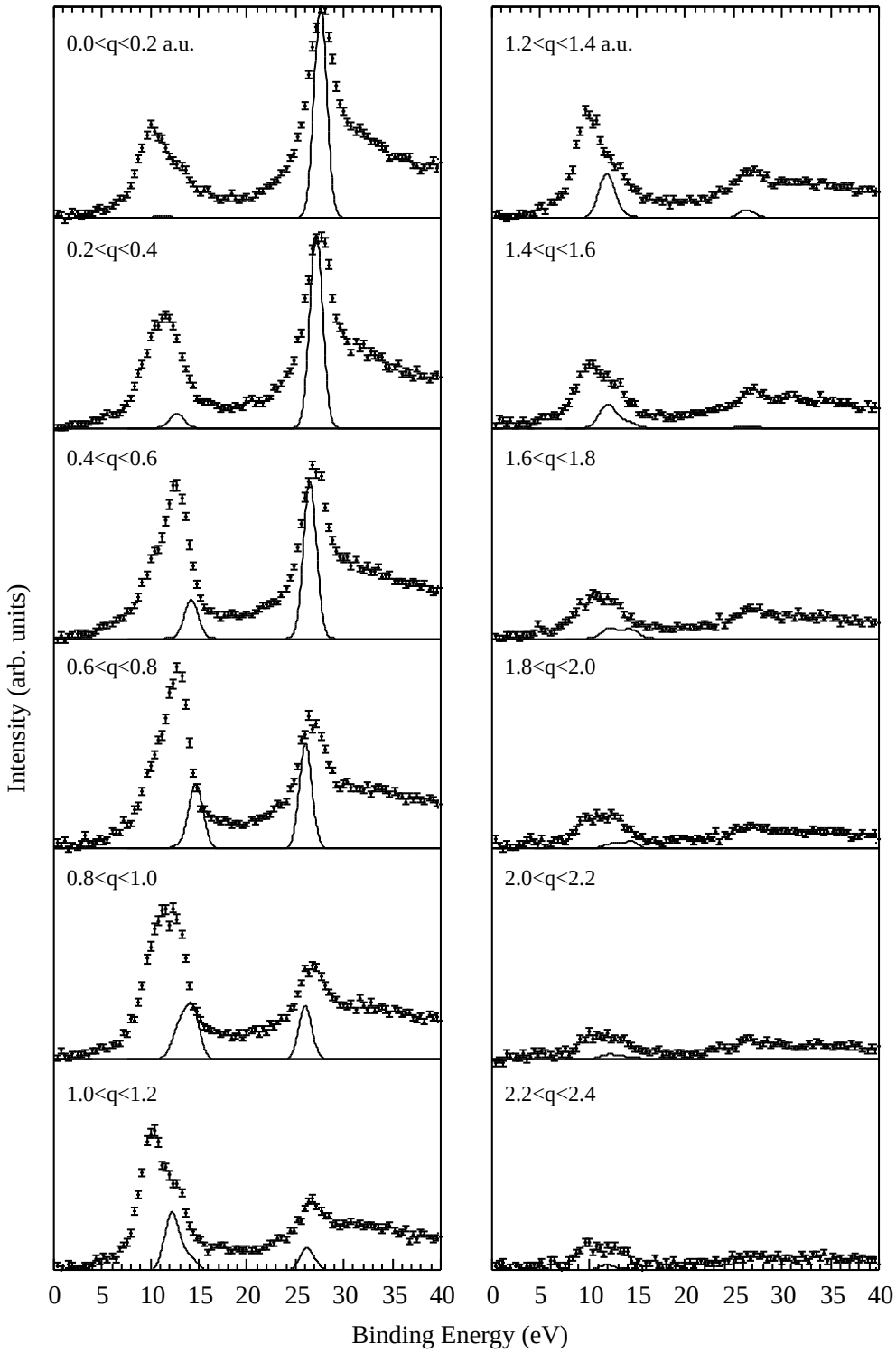

Figure 8. Binding energy profiles for MgO averaged over 0.2 au momentum intervals for the EMS measurement (points with error bars) and the LMTO calculation (solid line).

the LMTO calculation. Similar discrepancies between EMS measurements and theory were found for aluminium oxide [15] and silicon dioxide [13]. Multiple scattering effects can also contribute to a spreading of the band intensity. If any of the three electrons involved in the (e,2e) reaction is elastically scattered then the effect is a spreading of intensity along the momentum axis. This was seen as a 'filling-in' of intensity inside the free-electron parabola for Mg. It seems reasonable that some of the excess intensity of the upper valence band in MgO at small momentum values could result from this process, although, looking at how the intensity in the LMTO calculation for Mg (figure 6) is affected by the inclusion of a Monte Carlo simulation, it seems extremely unlikely that this mechanism can create a peaklike feature and account for all the excess intensity observed in the MgO upper valence band.

The measured inter-band gap reaches a minimum value of about 14 eV in the momentum interval $0.6 < q < 0.8$ au, whilst the minimum value from the spherically averaged LMTO calculation is approximately 11 eV. It was reported by Ochs *et al* [3] that the electronic structure of magnesium oxide prepared by evaporation of magnesium in an oxide environment is essentially the same as that of single-crystal MgO. However, the band gaps in figure 4 along any of the three high symmetry directions do not differ significantly from the spherically averaged value. Band gap values for single-crystal MgO of 11 eV and 10.6 eV have been reported by French *et al* [28], using the pseudofunction method, and Schönberger *et al* [6], using the LMTO–ASA method, respectively. The measured band gap is clearly at odds with our calculated value and those previously reported.

As mentioned previously a major difference between the metallic magnesium (figure 5) and insulating magnesium oxide (figure 7) measurements is the lack of a multiple scattering background in the latter. For the Mg results, although the free-electron parabola can clearly be seen above the background, there is substantial intensity at higher binding energies resulting from inelastic scattering events such as plasmon excitation. The MgO results on the other hand display minimal intensity between the upper and lower valence bands and also much less intensity at higher binding energies compared with Mg. To investigate further the contribution of inelastic multiple scattering we measured electron energy loss spectra for both the Mg and MgO samples. In these experiments the incident beam energy was tuned to the energy of the fast electron analyser (19.6 keV). The results are shown in figure 9. Both the Mg and MgO results are normalized to the same elastic peak height. The magnesium energy loss spectrum shows a sharp bulk plasmon peak at 10.5 eV, together with a surface plasmon peak at approximately 7.5 eV. These values agree well with other experiments, see for example Egerton [29]. The energy loss spectrum for MgO shows a much broader, less intense, plasmon peak around 22 eV; Henrich *et al* [30] report a value of 22.2 eV. The much smaller multiple scattering background observed in the energy–momentum density for MgO (figure 7(a)) compared with Mg (figure 5(a)) may partly result from the different intensity distributions of the plasmon peaks in figure 9. It must be remembered, however, that the energy–momentum densities are measured by coincidence detection of both the fast and slow outgoing electrons, so that excitation of plasmons by the slow ejected electron will also contribute to the measured background.

5. Conclusion

We have measured the full energy and momentum resolved electronic structure of Mg and MgO using electron momentum spectroscopy and compared these results to band structures calculated within the linear muffin-tin orbital approximation. As expected, we observe band structures which are characteristic of a metallic and ionic solid respectively: the calculation reproduces the structures at these two extremes of chemical bonding relatively well.

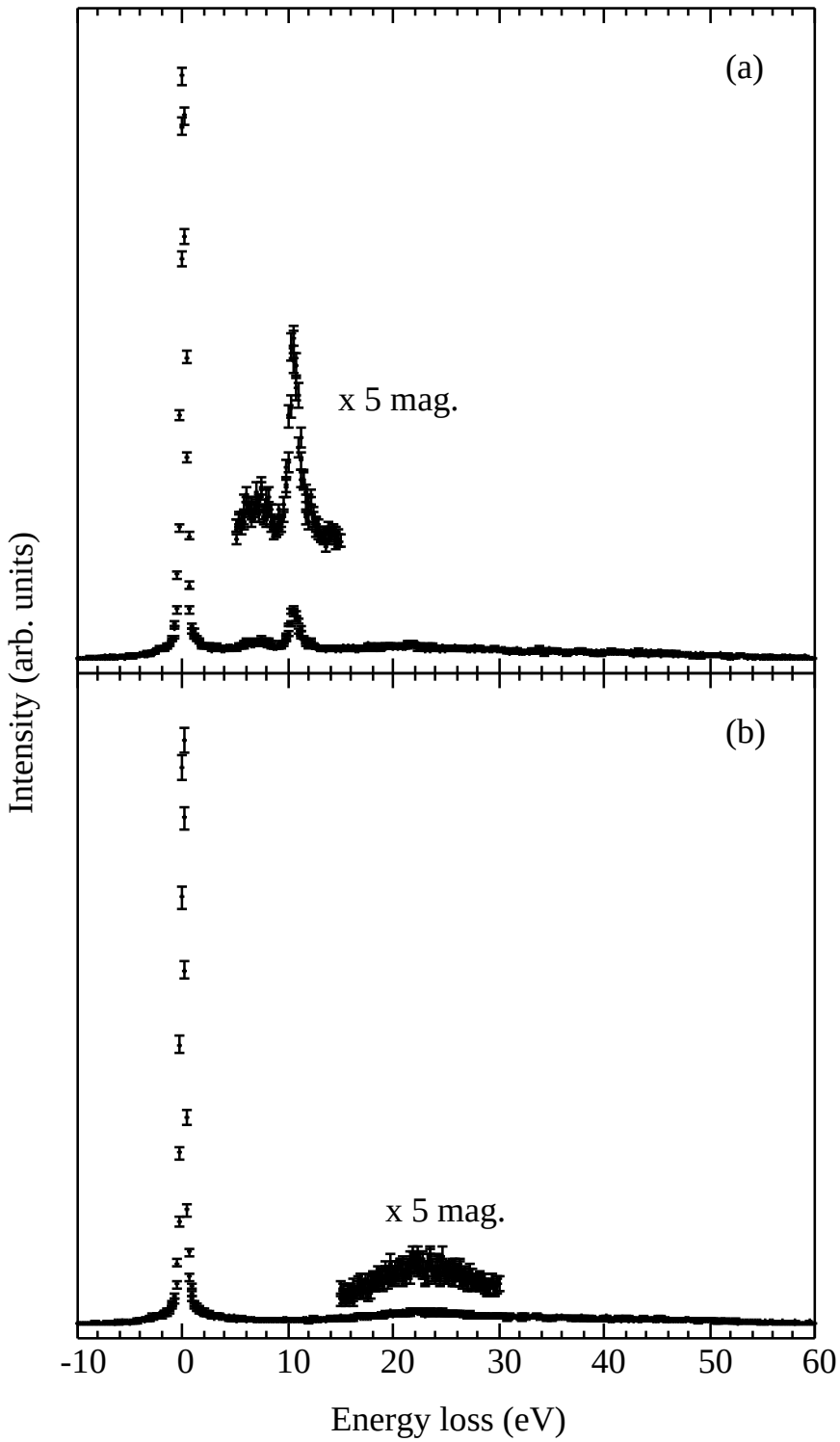

Figure 9. Electron energy loss spectrum with nominally 19.6 keV incident electron energy and electrons detected at 13.6° scattering angle for (a) Mg and (b) MgO.

In the case of Mg we find that the inclusion of lifetime broadening effects and multiple scattering events in the calculation gives good quantitative agreement with experiment. The observed valence bandwidth is in agreement with previous experiments and our LMTO calculation. Even after including multiple scattering events in the calculation using a Monte Carlo procedure, the predicted intensity at higher binding energies is still approximately 2 to 2.5 times lower than that observed. Either our Monte Carlo simulation is inadequate or correlation effects play an important role in Mg. It is expected that correlation should be important in Mg and it would be informative to compare our measurement to calculations that include correlation beyond the single-particle approximation.

Only qualitative agreement is found in the case of MgO. The observed width of the valence band peaks in our binding energy spectra are much larger than the calculation convoluted with the experimental resolutions and indicates that lifetime effects might play a significant role. The electron energy loss spectra show that plasmon excitation is very weak in MgO compared with Mg, as expected in an ionic solid, and may result in the small multiple scattering background observed for the oxide. There is disagreement between theory and experiment for both the inter-band gap and relative intensities of the upper and lower valence bands. Multiple scattering events can cause a redistribution of the band intensities, but we suspect not to the extent that is observed. We ascribe this difference to the fact that the LMTO calculation does not adequately describe the upper valence band at small momentum values. In the future we intend to investigate further this discrepancy in the band intensities by extending our Monte Carlo procedure to MgO in order to take account of multiple scattering. We also intend to compare our measurements with other calculation schemes to see whether they provide improved agreement with the observed band intensities and band gap.

Acknowledgments

This work was supported by grants from the Australian Research Council and Flinders University. The authors acknowledge Professor I E McCarthy for providing the scattering cross-sections used in the Monte Carlo procedure.

References

[1] Fuggle J C 1977 *Surf. Sci.* **69** 581
[2] Tjeng L H, Vos A R and Sawatzky G A 1990 *Surf. Sci.* **235** 269
[3] Ochs D, Maus-Friedrichs W, Brause M, Günster J, Kempter V, Puchin V, Shluger A and Kanotorovich L 1996 *Surf. Sci.* **365** 557
[4] Chang K J and Cohen M L 1984 *Phys. Rev.* B **30** 4774
[5] Causa M, Dovesi R, Pisani C and Roetti C 1986 *Phys. Rev.* B **33** 1308
[6] Schönberger U and Aryasetiawan 1995 *Phys. Rev.* B **52** 8788
[7] Karlsson U O, Hansson G V, Persson P E S and Flödstrom S A 1982 *Phys. Rev.* B **26** 1852
[8] Leckey R, Riley J, Cai Y, Faul J and Ley L 1993 *Aust. J. Phys.* **46** 717
[9] Leckey R and Riley J 1990 *Aust. J. Phys.* **43** 651
Leckey R and Riley J 1995 *Aust. J. Phys.* **48** 217
[10] Coplan M A, Moore J H and Doering J P 1994 *Rev. Mod. Phys.* **66** 985
McCarthy I E and Weigold E 1991 *Rep. Prog. Phys.* **54** 789
[11] McCarthy I E and Weigold E 1988 *Rep. Prog. Phys.* **51** 299
[12] Dennison J R and Ritter A L 1996 *J. Electron. Spectrosc. Relat. Phenom.* **77** 99
Vos M and McCarthy I E 1995 *J. Electron. Spectrosc. Relat. Phenom.* **74** 15
Fang Z, Matthews R S, Utteridge S, Vos M, Canney S A, Guo X, McCarthy I E and Weigold E 1998 *Phys. Rev.* B **57** 12 882
[13] Fang Z, Guo X, Canney S A, Utteridge S, Ford M J, McCarthy I E, Kheifets A S, Vos M and Weigold E 1998 *Phys. Rev.* B **57** 4349

[14] Canney S A, Vos M, Kheifets A S, Clisby N, McCarthy I E and Weigold E 1997 *J. Phys.: Condens. Matter* **9** 1931
[15] Guo X, Canney S, Kheifets A S, Vos M, Fang Z, Utteridge S, McCarthy I E and Weigold E 1996 *Phys. Rev.* B **54** 17 943
[16] Storer P, Caprari R S, Clark S A C, Vos M and Weigold E 1994 *Rev. Sci. Instrum.* **65** 2214
Canney S A, Brunger M J, McCarthy I E, Storer P J, Utteridge S, Vos M and Weigold E 1997 *J. Electron. Spectrosc. Relat. Phenom.* **83** 65
[17] Corneille J S, He J W and Goodman D W 1994 *Surf. Sci.* **306** 269
[18] Splinter S J, McIntyre N S, Lennard W N, Griffiths K and Palumbo G 1993 *Surf. Sci.* **292** 130
[19] Skriver H L 1984 *The LMTO Method* (Berlin: Springer)
[20] Wyckoff R 1963 *Crystal Structures* (New York: Interscience)
[21] Bartynski R A, Gaylord R H, Gustafsson T and Plummer E W 1986 *Phys. Rev.* B **33** 3644
[22] Vos M and Bottema M 1996 *Phys. Rev.* B **54** 5946
[23] Kimball C, Stark R W and Mueller F M 1967 *Phys. Rev.* **162** 600
[24] Gupta R D and Freeman A J 1976 *Phys. Rev. Lett.* **36** 1194
[25] Wilk L, Fehler W R and Vosko S H 1978 *Can. J. Phys.* **56** 266
[26] Vos M, Kheifets A S, Weigold E, Canney S A, Holm B, Aryasetiawan F and Karlsson K 1999 *J. Phys.: Condens. Matter* **18** 3645
[27] Henrich V E and Cox P A 1994 *The Surface Science of Metal Oxides* (Cambridge: Cambridge University Press)
[28] French R H, Kasowski R V, Ohuchi F S, Jone D J, Song H and Coble R L 1990 *J. Am. Ceram. Soc.* **73** 3195
[29] Egerton R F 1986 *Electron Energy Loss Spectroscopy in the Electron Microscope* (New York: Plenum)
[30] Henrich V E, Dresselhaus G D and Zeiger H J 1980 *Phys. Rev.* B **22** 4764